Supporting Information

Inducing a Transient Increase in Blood Brain Barrier Permeability for Improved Liposomal Drug Therapy of Glioblastoma Multiforme

David J. Lundy[†,‡], Keng-Jung Lee[†], I-Chia Peng[†], Chia-Hsin Hsu[†], Jen-Hao Lin[†], Kun-Hung Chen[†], Yu-Wen Tien[§] and Patrick C.H. Hsieh[†,§,∥,⊥,*]

[†]Institute of Biomedical Sciences, Academia Sinica, Taipei 115, Taiwan.

[‡]Graduate Institute of Biomedical Materials and Tissue Engineering, Taipei Medical University, Taipei 110, Taiwan.

[§]Department of Surgery, National Taiwan University and Hospital, Taipei 100, Taiwan.

[∥]Institute of Medical Genomics and Proteomics, National Taiwan University, Taipei 100, Taiwan.

[⊥]Institute of Clinical Medicine, National Taiwan University, Taipei 100, Taiwan.

Two methods

Three tables

Thirteen figures

Supplemental Methods

Antibody administration method. 30 µl Anti-NrCAM primary antibody (Abcam) was injected *via* tail vein, 45 minutes after VEGF or control administration. The antibody was allowed to circulate for 2 hours, then mice were perfused with 50 mL saline followed by 50 mL paraformaldehyde (4 % w/v). The brain was removed, kept in 4 % PFA overnight, then processed for frozen sections. As a positive control, 5 µl of antibody was injected directly into the brain prior to perfusion. Frozen sections were then stained using secondary antibody conjugated to Alexa 488. As a negative control, brain sections from an untreated animal were used. As a second positive control, a brain section from an untreated animal was stained with anti-nrCAM using conventional lab techniques (1hr room temperature). All images, aside from the stained positive control, were taken at fixed exposure lengths. The intensity of the green channel was quantified in ImageJ.

Assay for Phosphorus Quantification. Phosphorus standards were made using Sigma P3869. 15 µl of samples were mixed with 450 µl 8.9N H_2SO_4, heated to 200˚C for 25 mins, cooled for 5 mins, 150 µl 10% (v/v) H_2O_2 was added, heated again at 200˚C for 30 mins. After cooling, 3.9 ml H_2O, 0.5 ml 2.5% (w/v) ammonium molybate tetrahydrate, 0.5 ml 10% (w/v) ascorbic acid were added and the solution was heated to 100˚C for 7 mins. After cooling, absorbance was measured at 820 nm by plate reader.[1]

Table S1. Properties of polystyrene nanoparticles with carboxyl (COOH) surface chemistry and following polyethylene glycol modification (PEG).

Size (nm)	**Surface chemistry**	**Diameter TEM (nm)**	**Diameter DLS (nm)**	**Zeta potential (mV)**	**PDI**
20	COOH	25.7 ± 2.4	34.6 ± 0.8	- 34.1 ± 2.0	0.08
20	PEG	28.2 ± 1.8	52.4 ± 8.9	- 1.0 ± 4.0	0.06
100	COOH	92.7 ± 2.1	105.4 ± 2.7	- 43.1 ± 2.2	0.04
100	PEG	95.0 ± 2.1	120.1 ± 4.0	- 1.4 ± 0.3	0.06
500	COOH	471.8 ± 5.3	471.8 ± 5.3	- 48.7 ± 0.3	0.05
500	PEG	482.8 ± 4.5	512.1 ± 6.0	- 1.2 ± 0.2	0.03

Solid core diameter was measured by transmission electron microscopy (TEM) and hydrodynamic diameter and zeta potential were measured using a Malvern Zetasizer. Numbers show the mean ± standard deviation.

Table S2. Properties of LipoDox.

Size (nm)	Zeta potential (mV)	PDI	Drug : lipid ratio
95.55 ± 30.16	- 1.53	0.180	0.1556 ± 0.001943 : 1

Size and Zeta potential were calculated using Malvern Zetasizer. Drug : lipid ratio was calculated using the Bartlett assay. Numbers show the mean ± standard deviation.

Table S3. Primer sequences used in quantitative real-time PCR.

Gene name (human/ mouse)	Name. Function	Gene ID	Forward sequence	Reverse sequence	Product length	Avg C_T (brain control)
GAPDH/Gapdh	GAPDH. Internal control	NM_001289726.1	ACC CAG AAG ACT GTG GAT GG	CAC ATT GGG GG T AGG AAC AC	171	18
Neuroinflammation markers						
TNF/Tnf	TNFα. Acute phase cytokine	NM_013693	GAC CCT CAC ACT CAG ATC ATC TTC T	CCT CCA CTT GGT GGT TTG CT	80	28
IL-1b/Il1b	IL-1β. Inflammatory cytokine	NM_008361	TGC CAC CTT TTG ACA GTG ATG	ATG TGC TGC TGC GAG ATT TG	136	31
IL6/Il6	IL-6. Acute phase cytokine	NM_031168	TCC AGA AAC CGC TAT GAA GTT C	CAC CAG CAT CAG TCC CAA GA	73	31
CCL2/ccl2	CCL2. Chemokine	NM_011333	GTT GGC TCA GCC AGA TGC A	AGC CTA CTC ATT GGG ATC ATC TTG	81	30
GFAP/Gfap	GFAP. Astrocyte marker	NM_001131020.1	GAA CAA CCT GGC TGC GTA TAG	GCG ATT CAA CCT TTC TCT CCA A	80	29
CXCL1/cxcl1	CXCL1. Chemokine	NM_008176	CAC CCA AAC CGA AGT CAT AGC	AAT TTT CTG AAC CAA GGG AGC TT	82	21
FN1/Fn1	Fibronectin 1	NM_010233	AGG CAA TGG ACG CAT CAC	CTC GGT TGT CCT TCT TG	104	24
IL-1a/Il1a	IL-1α. Acute phase cytokine.	NM_010554	CGC TTG AGT CGG CAA AGA AAT C	CAG AGA GAG ATG GTC AAT GGC A	115	31
BBB components						
TFR/Tfrc	Transferrin receptor	NM_011638	CTG CTC ATC ACT ATG GTG GCT A	TGA CCC CAT GGC AAA ACT GA	108	27
CRT/Slc6a8	Creatinine transporter	NM_133987.2	GTG GGG GTA AGG GTG GAA TGT A	GCC ACA ACT ACA CAC TCC CAA	103	33
GLUT1/Slc2a1	Glucose transporter	NM_011400.3	TGG CGG GAG ACG CAT AGT TA	GCC CGT CAC CTT CTT GCT	110	24
ATA2/Slc38a2	Amino acid transporter	NM_175121.4	ACG AAA CAG ACT TTC ATC CAG GTA	AAG CCC AAG GAT TCC ACT GC	92	23
MRP4/Abcc4	Multidrug resistance pump	NM_001163676.1	GGG CGA GAT GCT GCC G	GGG TTG AGC CAC CAG AAG AA	93	30
MDR1a/Abcb1a	P-glycoprotein efflux pump	NM_011076.2	CCA TCT TCC AAG GCT CTG CT	CCA TCA CGA CCT CAC GTG TC	107	26
ZO1/Tjp1	Tight junction protein	NM_009386.2	CCT GTG AAG CGT CAC TGT GT	CGC GGA GAG AGA CAA GAT GT	100	25

ZO2/Tjp2	Tight junction protein	NM_001198985	GAGATGCCGGTGCGGG	TTTGGAATCCTTCTGCAGGG	126	27
OCLN/Ocln	Tight junction protein	NM_008756.2	CAT AGT CAG ATG GGG GTG GA	ATT TAT GAT GAA CAG CCC CC	91	26
CLDN5/Cldn5	Tight junction protein	NM_013805.4	GTC ACG ATG TTG TGG TCC AG	AAA TTC TGG GTC TGG TGC TG	106	25
JAM-A/F11r (CD321)	Tight junction protein	NM_172647.2	AGT GTA CAC CGA ACC CTT GC	TGT AAC TGT AAT GGG CAC CG	106	27
SPARC1/Sparcl 1	ECM adhesion	NM_010097.4	ACC TCT CCG CAG ATC TAG CCA	GGT GTC ACC AGT GTT GCA GT	136	20
MAOB/Maob	Enzymatic barrier	NM_172778.2	GCT GGA CCA AAT CTA CAA AGC A	TGG TTG TAC CTC CAC ACT GC	123	26

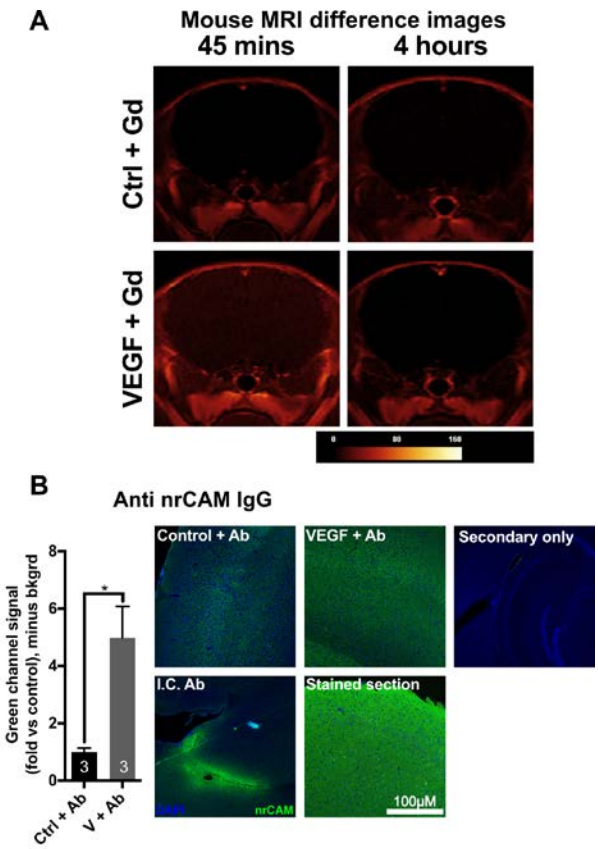

Fig. S1. Supporting MRI images and penetration of IgG antibody into the brain.

A) Difference image of mouse MRI. B) Penetration of anti-nrCAM IgG primary antibody into brain tissue. Primary antibody was injected intravenously, 45 minutes following control or VEGF, then the animal was perfusion fixed, the brain was frozen sectioned, and stained with fluorescent secondary antibody. For the I.C. Ab sample, anti-nrCAM was directly injected intracranially. A section stained by conventional methods is also shown for reference.

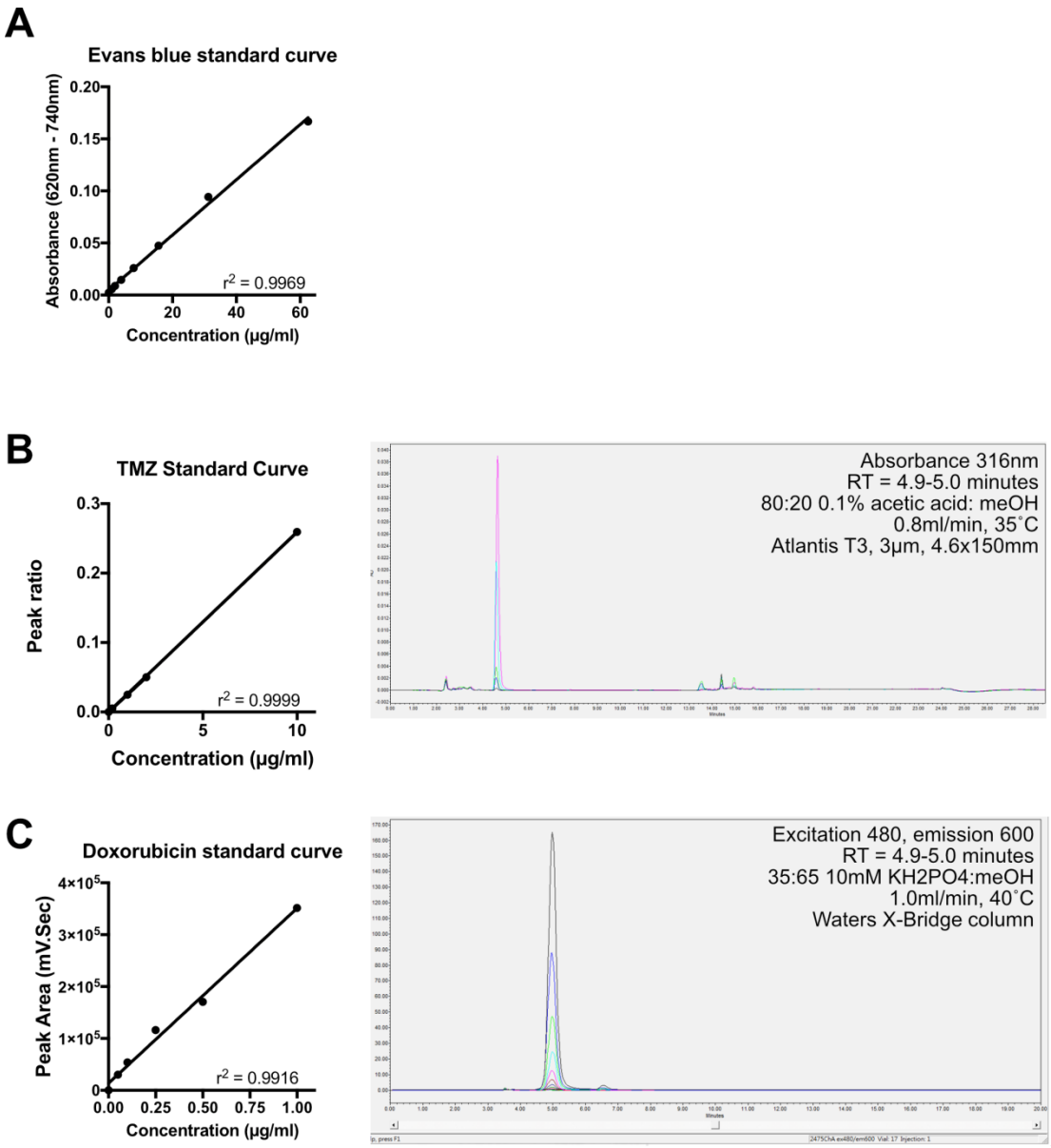

Figure S2. Standard curves for Evans blue, TMZ and Doxorubicin.

Standard curves for **(A)** Evans blue (plate reader), **(B)** Temozolomide and **(C)** Doxorubicin (HPLC). Example HPLC peaks are shown, along with HPLC operating conditions.

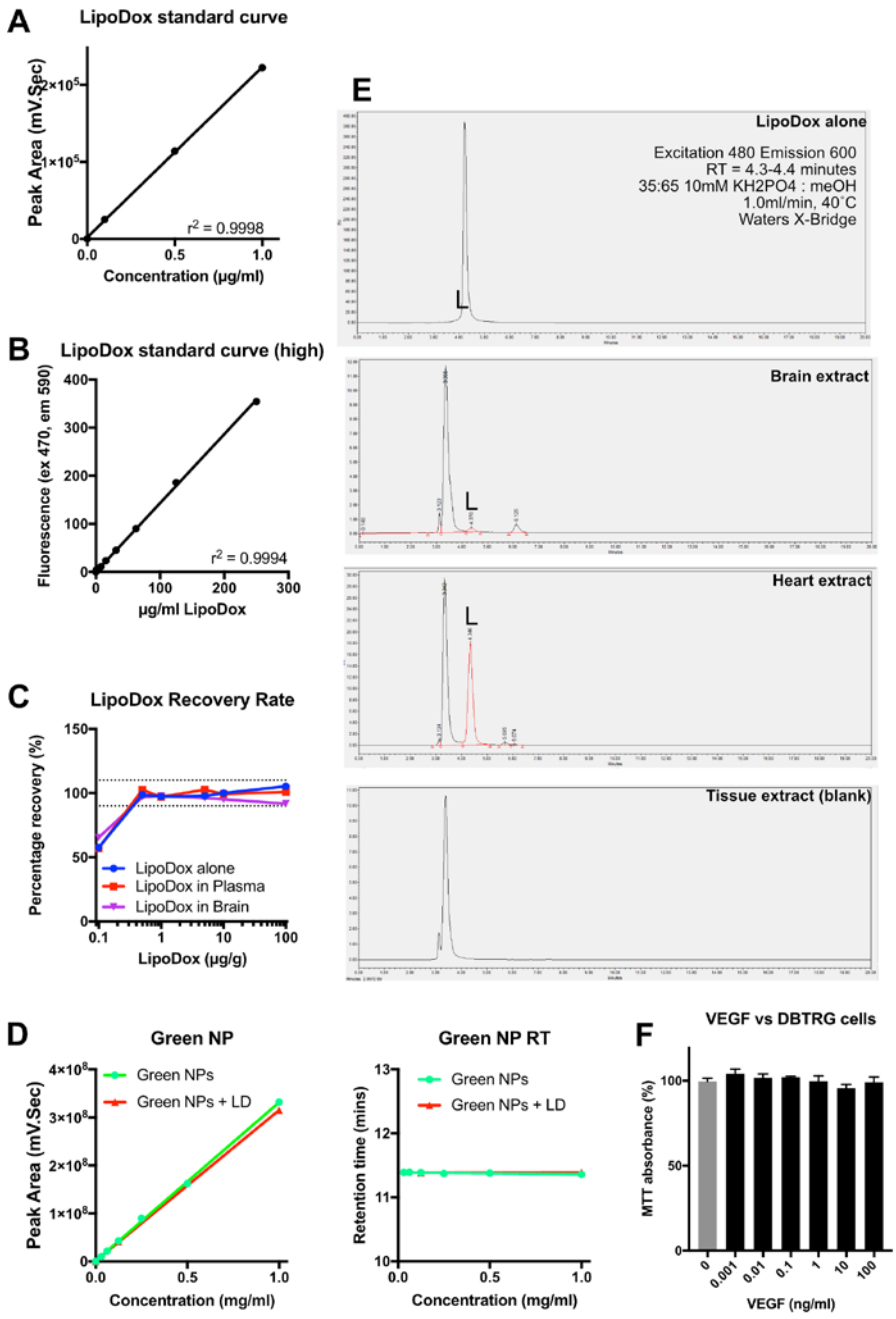

Figure S3. LipoDox and nanoparticle HPLC quantification.

(**A**) Standard curve of low concentration (< 1.0 µg/ml) LipoDox. (**B**) Standard curve of high concentration (< 300.0 µg/ml) LipoDox. (**C**) LipoDox recovery from brain tissue. Dotted lines indicate 90 % and 110 % margins. (**D**) Standard curve of HPLC-based nanoparticle quantification, with and without the presence of LipoDox. The right side graph shows that presence of LipoDox does not affect nanoparticle dye retention time. (**E**) Example HPLC peaks showing blank tissue, LipoDox extracted from brain and heart, and LipoDox alone. The LipoDox peak is marked by "L". (**F**) MTT assay showing DBTRG cells cultured with VEGF up to a concentration of 100 ng/ml.

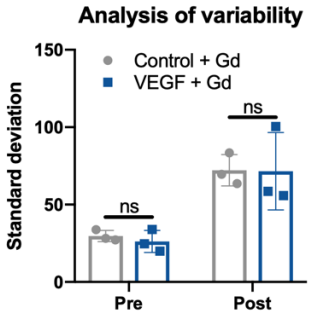

Figure S4. Quantification of variation in pig MRI signal enhancement.

Graph showing standard deviations of SNR enhancement. An ROI was drawn to encompass the brain parenchyma, excluding the ventricles. For “pre” images, the difference between two pre-contrast images were analysed, to establish a baseline amount of variation which occurs between sequential images.

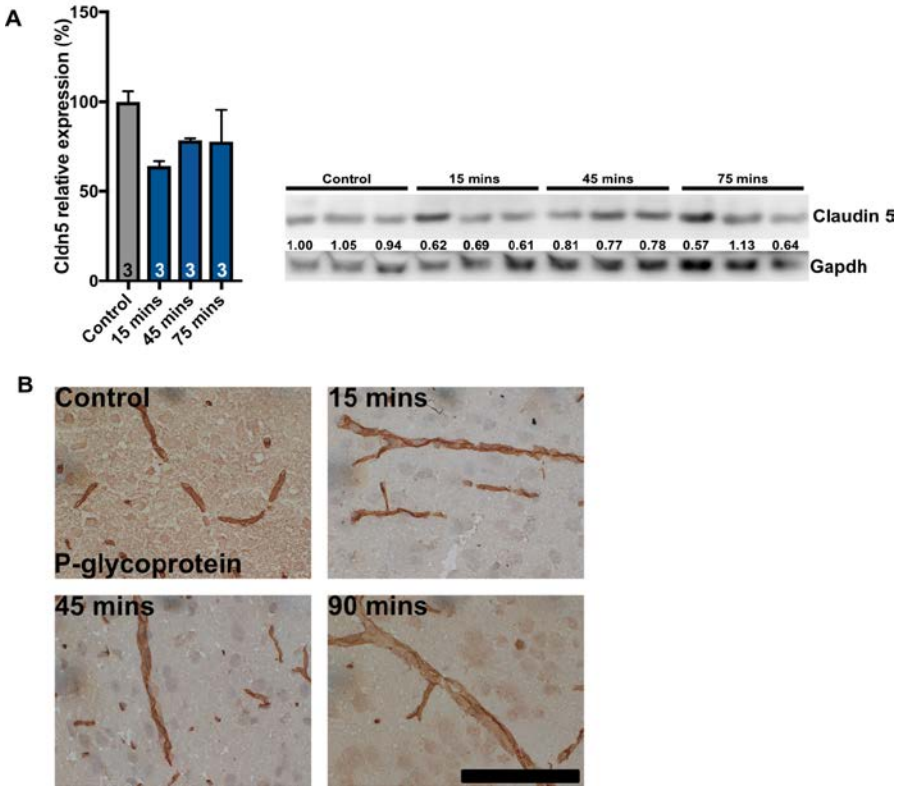

Figure S5. Western blot of claudin 5. P-glycoprotein staining.

(**A**) Western blot of whole mouse brain Claudin 5 following VEGF treatment. (**B**) P-glycoprotein staining following VEGF treatment. Scale bar = 100 µm.

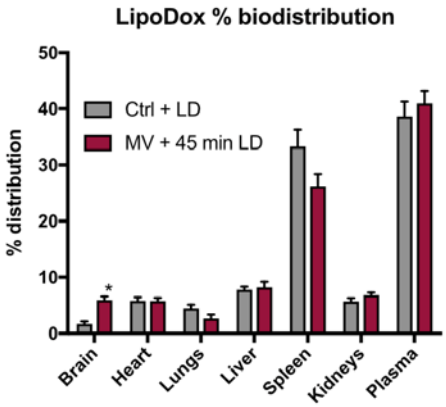

Figure S6. Biodistribution of LipoDox following MV + LD treatment in mice.

Biodistribution of LipoDox following multi-VEGF and LipoDox administration. Biodistribution expressed as percentage of LipoDox recovered.

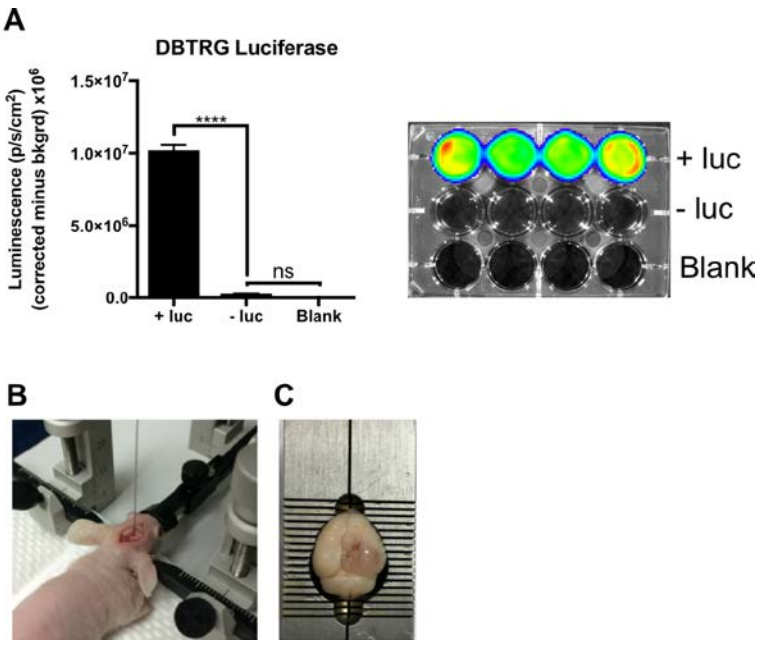

Figure S7. Further GBM model information.

(**A**) Luciferase expression of engineered DBTRG-05MG human glioblastoma cell line. (**B**) Example of BALB/c NU mouse receiving intracranial injection. (**C**) Typical tumour morphology in right hemisphere after 65 days.

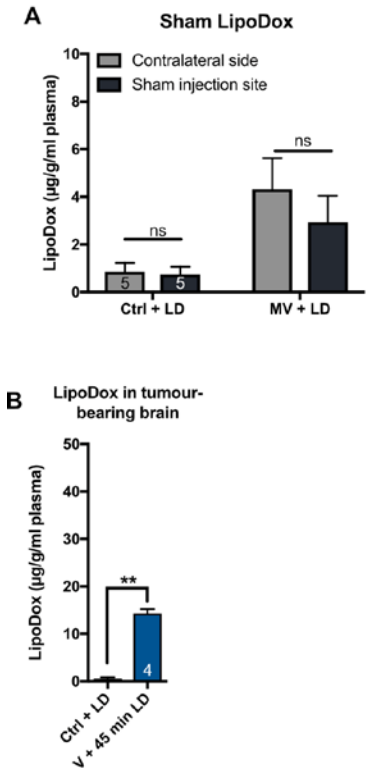

Figure S8. Effect of sham injections on drug retention. Intratumoral LipoDox following V + LD treatment.

(**A**) LipoDox concentration at the sham injection site or contralateral side in mice. (**B**) Intratumoural LipoDox concentration following a single dose of VEGF followed by LipoDox.

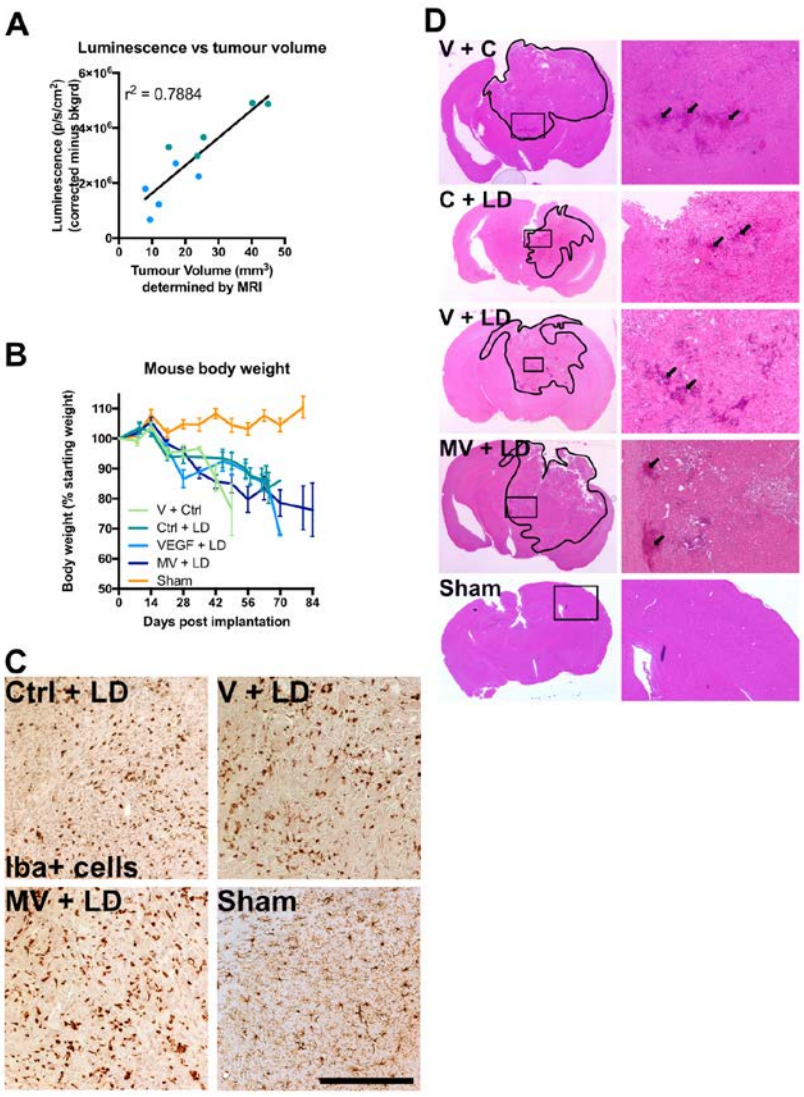

Figure S9. Mouse body weights, Iba1 tumour staining, example tumour H&E image.

(**A**) Correlation of tumour luminescence determined by IVIS vs confirmed tumour size by MRI. (**B**) Mouse body weight throughout survival experiment. (**C**) Iba1 staining of tumours from mice in treatment groups. The corresponding normal brain region was imaged in the sham mice. Scale bar = 100 µm. (**D**) Composite example H&E stained brain slices from tumour-bearing mice. The tumour region is outlined and a magnified view is presented. Areas of haemorrhage are indicated with black arrows. The haemorrhage area was calculated as a percentage of the tumour area.

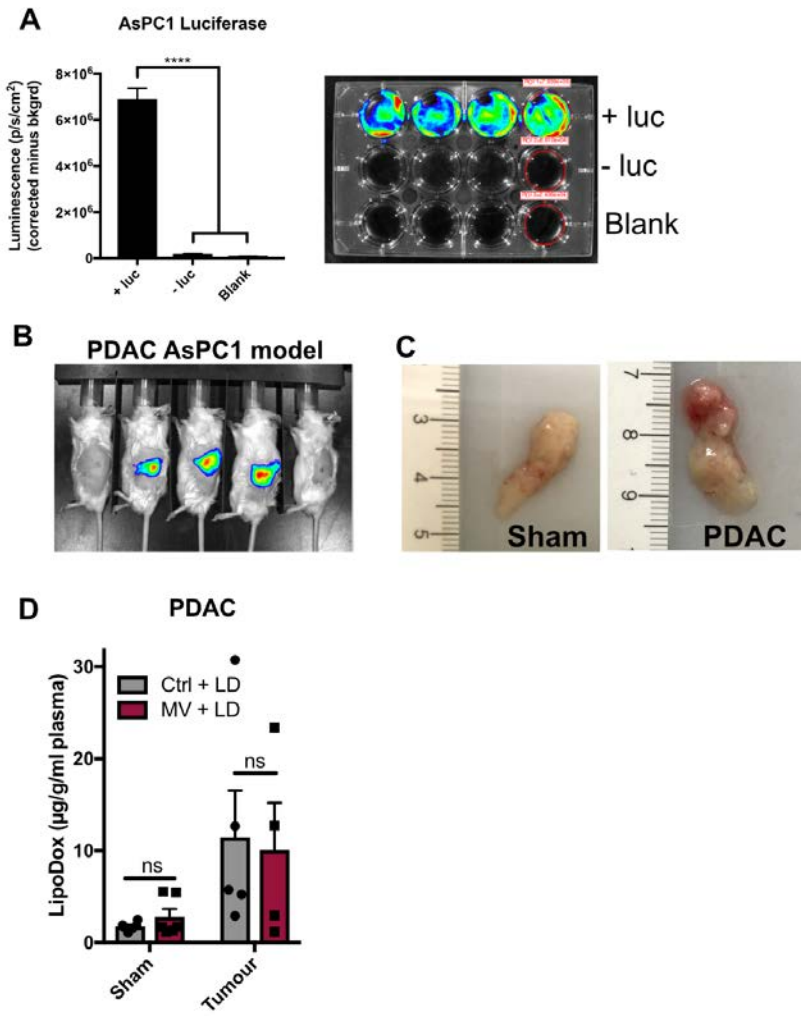

Figure S10. PDAC model information.

(**A**) IVIS confirming luciferase expression of AsPC1 cells. (**B**) IVIS showing pancreatic tumour establishment in mice. (**C**) Example photo of normal pancreas and PDAC xenograft pancreas. (**D**) Quantification of LipoDox in PDAC tumours or sham-operated pancreas.

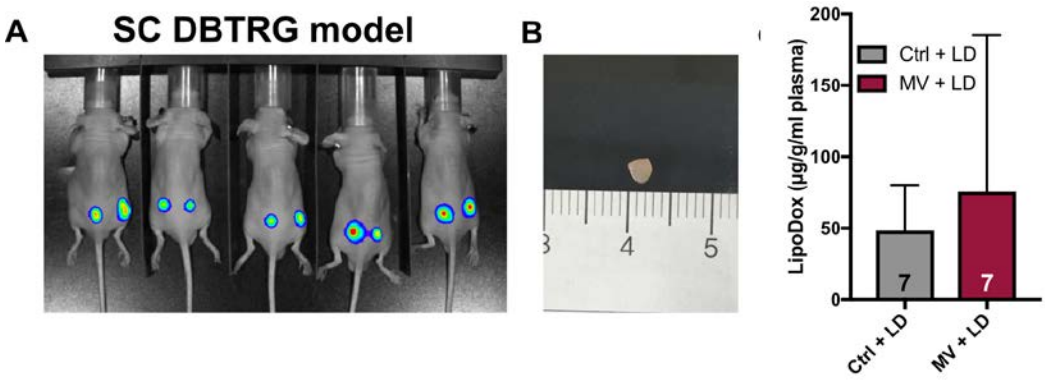

Figure S11. Subcutaneous GBM model information.

(**A**) Representative IVIS image of subcutaneous (SC) tumour growth. (**B**) Representative tumour after 60 days. (**C**) Intratumoural LipoDox concentration following control or VEGF pre-treatment.

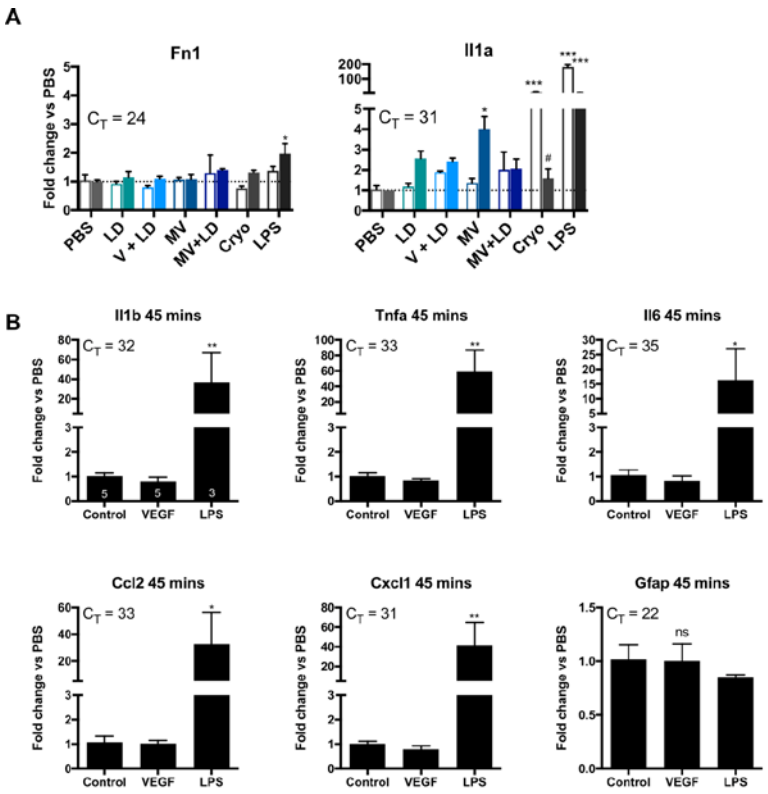

Figure S12. Supplementary 45 minute, 4 hr and 24 hr inflammation gene expression.

(**A**) Expression of Fn1 and Il1a following treatment groups. Cryolesion (cryo) and lipopolysaccharide (LPS) were used to induce neuroinflammation as positive controls. (**B**) Gene expression 45 minutes following VEGF administration. Error bars show standard error of the mean. Inset numbers indicate the number of animals. * $p < 0.05$, ** $p < 0.01$, *** $p < 0.001$, **** $p < 0.0001$ compared to control. ns indicates not significant.

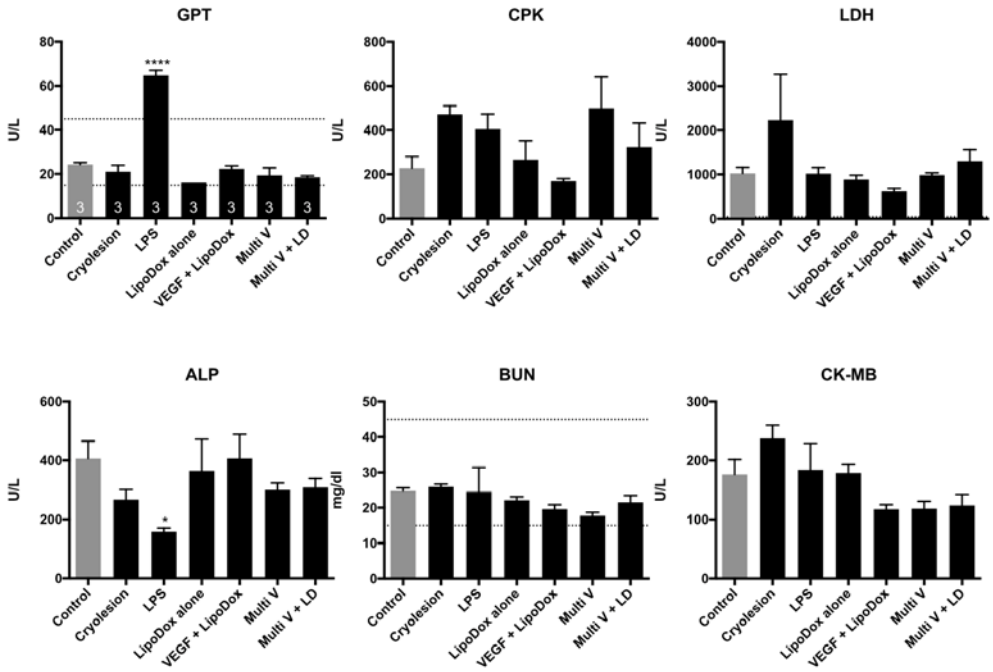

Figure S13. Mouse serum blood chemistry.

ALT/GPT, alanine Aminotransferase; CPK, creatinine kinase; ALP, alkaline phosphatase; BUN, blood urea nitrogen; LDH, lactate dehydrogenase; CK-MB, creatinine kinase MB.

Dotted lines show internal laboratory references ranges, where available.

Supplemental references

(1) Bartlett, G. R. Colorimetric Assay Methods for Free and Phosphorylated Glyceric Acids. *J Biol Chem* **1958**, *234*, 469–471.